Progress in Physics of Applied Materials 6 (2026), Serial Number 12, 249-255

Semnan University

Progress in Physics of Applied Materials

journal homepage: https://ppam.semnan.ac.ir/

Binder-Free Mesoporous Vanadium Oxide Electrode: Anodic Electrodeposition, Characterization, and Supercapacitor Application

Mahdi Kazazi *, **Soheila Kazemi**, **Behzad Koozegar Kaleji**

Department of Materials Engineering, Faculty of Engineering, Malayer University, Malayer, Iran

ARTICLE INFO

Article history:
Received: 1 January 2026
Revised: 7 February 2026
Accepted: 9 February 2026
Published online: 11 March 2026

Keywords:
Vanadium oxide;
Mesoporous structure;
Electrodeposition;
Binder-free electrode;
Supercapacitors.

ABSTRACT

Mesoporous vanadium oxide (V_2O_5) was galvanostatically electrodeposited into nickel foam to obtain a binder-free electrode with a three-dimensional (3D) porous structure for supercapacitive performance. The anodic electrodeposition process was performed using an aqueous solution of vanadyl sulfate, which was completed by calcination treatment. XRD and FTIR confirmed the formation of the orthorhombic V_2O_5 structure, also and FESEM and BET analysis revealed the 3D mesoporous structure of the electrode material. The supercapacitive performance of the fabricated electrode was evaluated using CV, GCD, and EIS examinations in lithium perchlorate electrolyte. The charge storage mechanism involved the intercalation/de-intercalation of lithium ions within the electrode structure, resulting in a vanadium valence shift between V^{4+}/V^{5+}. The prepared electrode showed an acceptable capacitance of 496 F g^{-1} at a rate of 1 A g^{-1}, a suitable rate performance with a capacitance retention of 36.1%, and good cyclability with a capacitance retention of 85.2% after 2000 cycles. The resulting porous structure shortens the diffusion path of electrolyte ions to the active material, while the removal of the insulating binder reduces its the internal resistance, both of which improve the kinetics of electrochemical reactions. These results demonstrate the promise of vanadium oxide as an advanced electrode material for next-generation high-performance energy storage devices.

1. Introduction

In today's life, energy production using fossil fuels is limited due to limited fossil fuel resources, air pollution, and global warming. On the other hand, the increasing energy demand has led humanity to use clean energy such as wind and solar energy. It should be noted that clean energy is intermittent and not always available. Therefore, these energy sources must always be accompanied by energy storage systems to ensure constant access to energy [1].

Compared to batteries, supercapacitors (SCs) can store energy at a faster rate, although their energy storage capacitance is lower. Therefore, SCs are frequently used in combination with batteries in electric vehicles to provide high-power energy during rapid acceleration, while the main source of energy for the vehicle is the batteries [2,3].

The storage mechanism in SCs is derived from two types of the electric double layer capacitance (EDLC) and pseudocapacitance charge storage by Faradic oxidation-reduction reactions. In EDLCs, energy is stored by separating the charge at the interface of the electrolyte and active material. These SCs have a very high charge-discharge rate, although their storage capacitance is limited. Various carbon materials are used as active materials in EDLCs due to their large specific surface area, high

* Corresponding author.
E-mail address: kazazi@malayeru.ac.ir; mahdi.kazazi@gmail..com

Cite this article as:

Kazazi, M., Kazemi, S. and Koozegar Kaleji, B., 2026. Binder-Free Mesoporous Vanadium Oxide Electrode: Anodic Electrodeposition, Characterization, and Supercapacitor Application. *Progress in Physics of Applied Materials*, *6*(3), pp.249-255. DOI: **10.22075/ppam.2026.40173.1198**

conductivity, and electrochemical neutrality. In contrast, electrochemical pseudocapacitors, such as batteries, store electric charge by performing Faradic reactions in the electrode materials. Conductive polymers and metal oxides/hydroxides/sulfides that have the characteristics of availability, non-toxicity, and suitable electrochemical activity can be used as active materials in pseudocapacitors. Transition metal oxides offer excellent pseudocapacitive performance through reversible redox reactions in a large potential window and in multiple oxidation states [4-7].

Among the types of transition metal oxides, vanadium oxide (V_2O_5) has attracted attention due to its low toxicity, cost-effectiveness, natural abundance, high theoretical capacitance (2120 F g^{-1}), and various states of oxidation (V^{2+}, V^{3+}, V^{4+}, and V^{5+}). However, the low diffusion rate of electrolyte ions into the V_2O_5 has caused major problems, such as low practical capacitance and inappropriate current rate capability. Synthesis of nanoscale active material with mesoporous characteristics that increase its surface area and greatly enhance ionic diffusion can significantly overcome the problem of the limited availability of V_2O_5 active material [8-12].

Traditionally, energy storage electrodes are prepared via coating a slurry consisting of an active material, a conductive agent, and a binder on the current collector surface. Unfortunately, the use of an insulating polymeric binder such as polyvinylidene fluoride (PVDF) or polytetrafluoroethylene (PTFE) in the fabrication of electrodes increases the internal resistance, leading to a drop in its their electrochemical performance. The use of binder-free electrode preparation methods like electrostatic spinning [13], chemical vapor deposition [14], vacuum infiltration [15], and electrochemical deposition [16] can overcome the problem of internal resistance of the electrode by eliminating the non-conductive binder. Among these methods, electrodeposition has attracted attention for the preparation of SC electrodes due to its advantages, such as cost-effectiveness, no need for special equipment, flexibility, and operating at low pressures and temperatures [17].

Energy storage electrodes in batteries and supercapacitors are fabricated by applying an active material to the surface of a neutral conductive substrate known as a current collector. Various current collectors, including graphite, carbon cloth, carbon paper, copper, aluminum, stainless steel, and nickel foam (NF), have been used in the fabrication of supercapacitor electrodes. It has been demonstrated that the use of current collectors with a three-dimensional (3D) structure, such as nickel foam, in addition to increasing the mass loading of the active material per unit area, provides a very effective accessibility for the active material, thereby enhancing the supercapacitor performance [18].

Herein, we developed an effective procedure for the fabrication of binder-free mesoporous V_2O_5 electrode based on anodic electrochemical deposition into the NF. The as-prepared electrode was carefully evaluated in terms of morphology, structure, specific surface area and pseudocapacitive performance using appropriate techniques.

2. Experimental

2.1. Preparation of 3D Nickel Foam Current Collector

In this study, to remove oxide layers from the NF surface, an acid pickling process was performed on this substrate. For this purpose, first, NF was cut into 1×1 cm^2, and then the substrates were ultrasonicated in 6M HCL solution for 30 minutes. Then, the current collectors were taken out from the acid solution and washed with abundant distilled water and ethanol, respectively, until the acid solution was completely eliminated from the pores of the nickel foam. Finally, the substrates were dried and kept in a desiccator until the electrochemical deposition process.

2.2. Anodic Electrochemical Deposition of Mesoporous V_2O_5

To prepare the electrolyte for the electrodeposition process, initially, 0.15 g of sodium sulfate (Na_2SO_4) was completely dissolved in 10 ml mixture of deionized water and ethanol (50:50), while stirring was continued by magnetic stirring. Finally, 1.0 g of $VOSO_4.xH_2O$ was added to the above solution and stirred until a uniform solution was formed.

For the electrochemical deposition of vanadium oxide, NF substrate was employed as the anode, and a 316L stainless steel sheet with a large surface area was employed as the cathode. The electrodeposition process was carried out under galvanostatic conditions at a current density of 30 mA cm^{-2} for 10 min at room temperature to form a relatively thick layer on the nickel foam substrate. Finally, the nickel foam was separated from the electrolyte, washed with distilled water, and dried with a hot air stream. To form the V_2O_5 phase, the coated nickel foams were calcined at 400°C for 2 h.

2.3. Structural Characterization and the Electrochemical Performance of the V_2O_5 Electrode

The structural analysis of the fabricated V_2O_5 electrode was performed using XRD (Unisantis XMD-300) in the range of 10-70° at a step size of 0.02°. To further investigate the structure and chemical bonds of the active material, an FTIR spectrophotometer (PerkinElmer) was identified in the range of 400-4000 cm^{-1}. Recognizing the critical role of surface properties in supercapacitor performance, detailed morphological studies were carried out using scanning electron microscopy (FESEM: Mira 3-XMU). The specific surface area and specific pore volume of the active material were measured using a nitrogen adsorption-desorption test at a temperature of -196°C via the BET method by a BELSORP-mini instrument (BEL, Japan Inc.). For this measurement, after the calcination process, the active material was scraped from the surface of the NF substrate to obtain V_2O_5 powder.

To consider the supercapacitive performance of the V_2O_5 electrode, a three-electrode cell containing a 2M $LiClO_4$ solution was used, in which the V_2O_5 electrode was employed as the working electrode, a standard Ag/AgCl was employed as the reference electrode, and a Pt sheet was employed as the counter electrode. Electrochemical evaluations were carried out using galvanostatic charge-discharge (GCD), cyclic voltammetry (CV), and electrochemical impedance spectroscopy (EIS) using an Autolab electrochemical workstation (PGSTAT204). EIS measurement was conducted over the frequency range of 100 kHz-100 mHz with the amplitude of the sinusoidal signal of ±10 mV at open circuit voltage (~-0.5 V vs. Ag/AgCl).

3. Results and Discussion

3.1. Electrode Characterization

It should be noted that the electrodeposition mechanism of vanadium oxide in vanadyl sulfate aqueous electrolyte is as follows [18]:

$$VOSO_4 \leftrightarrow VO^{2+} + SO_4^{2-} \quad (1)$$

$$2VO^{2+} + 3H_2O \rightarrow V_2O_5 + 6H^+ + 2e^- \quad (2)$$

The electrodeposition mechanism of vanadium oxide, according to reactions (1) and (2) includes two steps. In the first step, the VO^{2+} species with V^{4+} valence is formed in the blue vanadyl sulfate solution. In the next step, this species is oxidized to V_2O_5 with a valence of V^{5+} on the anode surface, which is deposited on the nickel foam surface with a dark green color.

In order to ensure the formation of the V_2O_5 phase and the formation or absence of side phases in the prepared vanadium oxide electrode, XRD analysis was performed. The XRD pattern of the powder scratched from the V_2O_5 electrode surface after calcination at 400°C displayed in Figure 1. As seen, the peaks at 2θ angles of 12.31, 15.49, 20.34, 21.82, 25.67, 31.13, 32.11, 33.56, 34.44, 40.11, 45.22, 46.99, 47.48, 49.11, 51.11, 51.78, 56.48, 58.23, 62.23, and 66.11° have been formed. These peaks respectively belong to the crystal planes of (001), (200), (001), (101), (110), (400), (011), (310), (211), (002), (411), (600), (302), (012), (020), (601), (021), (412), (710), and (800), all of which are related to the orthorhombic structure of vanadium oxide (V_2O_5). The position and intensity of these peaks correspond to the JCPDS standard pattern No. 89-0612, which indicates the high purity of the V_2O_5 phase in the electrode [19].

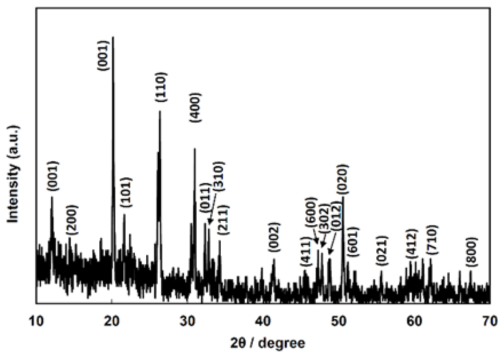

Fig. 1. XRD pattern of the V_2O_5 electrode.

Various functional groups present in the V_2O_5 active material were investigated via FTIR spectroscopy. Figure 2 depicts the spectrum obtained for the V_2O_5 electrode after calcination at 400°C. The broad band observed at 3449 cm^{-1} is related to the stretching of the O–H due to the adsorbed H_2O. The observed bands at the wave numbers of 520, 590 and 662 cm^{-1} are related to the stretching of oxygen-metal bonds, especially the symmetric V–O–V and V–O stretching modes. The peaks in the range of 950 to 1110 cm^{-1} are attributed to the stretching vibrations related to the vanadyl (δ V–O) bond and the V=O double bond. Also, bands in the range of 1105 to 1400 cm^{-1} are observed, which could be due to the asymmetric stretching of the V=O bond [20].

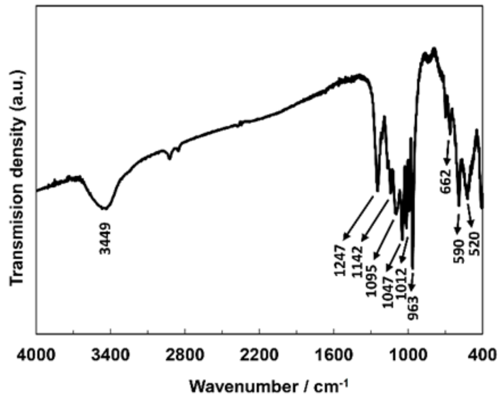

Fig. 2. FTIR spectrum of V_2O_5 sample scratched from the electrode surface.

Considering that the surface area and porosity of the active material have a considerable effect on the kinetics of energy storage reactions, the surface area and the pore volume of the powder scratched from the V_2O_5 electrode were measured. Figure 3 illustrates the adsorption and desorption isotherms of nitrogen at -196°C for the V_2O_5 active material. It can be observed that the sample exhibits the classical shape of a type IV isotherm according to the IUPAC classification, typical for a mesoporous structure. The existence of the hysteresis loop in the isotherms is due to the capillary condensation of N_2 gas occurring in the mesopores. The presence of a hysteresis loop of type H1 in the relatively high-pressure region (P/P0=0.45-1) indicates its mesoporous structure. Using the BET method, the specific surface area for the V_2O_5 active material was equal to 20.9 m^2 g^{-1}, and the specific total pore volume was equal to 0.053 cm^3 g^{-1}. The existence of a mesoporous structure with a high specific surface area shortens the diffusion path of electrolyte ions towards the electrode material, and enhanced electrochemical characteristics are expected. This increases the practical capacitance and improves the performance rate of the electrode.

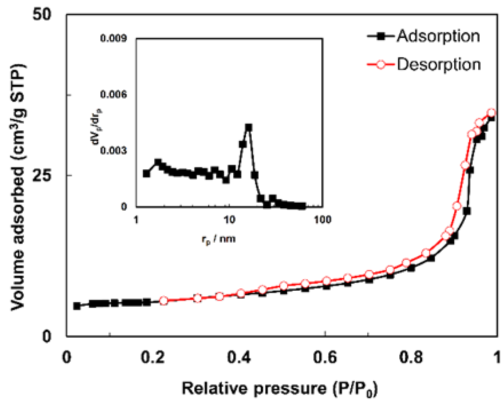

Fig. 3. Nitrogen adsorption-desorption isotherm for the V_2O_5 electrode material.

A supercapacitor is a surface phenomena in which surface morphology and porosity plays an important role in ion adsorption and intercalation/ de-intercalation kinetics. Hence, to study surface topographical aspects of calcinated product, field emission scanning electron microscope (FESEM) technique was used and those results are shown in Figure 4. As seen in Figure 4a, the NF blades are uniformly covered by the V_2O_5 active material, and the nickel foam cavities are not filled to allow the electrolyte to penetrate into the nickel foam structure. Also, a 3D porous structure has been formed, in which the thickness of blades is in nanometric dimensions. The obtained unique 3D mesoporous structure is very attractive for energy storage systems, because it allows easy access of charge and ions to the electrode material. This unique structure, while increasing the electrochemical use of the electrode material, facilitates the kinetics of electrochemical reactions and increases its practical capacitance.

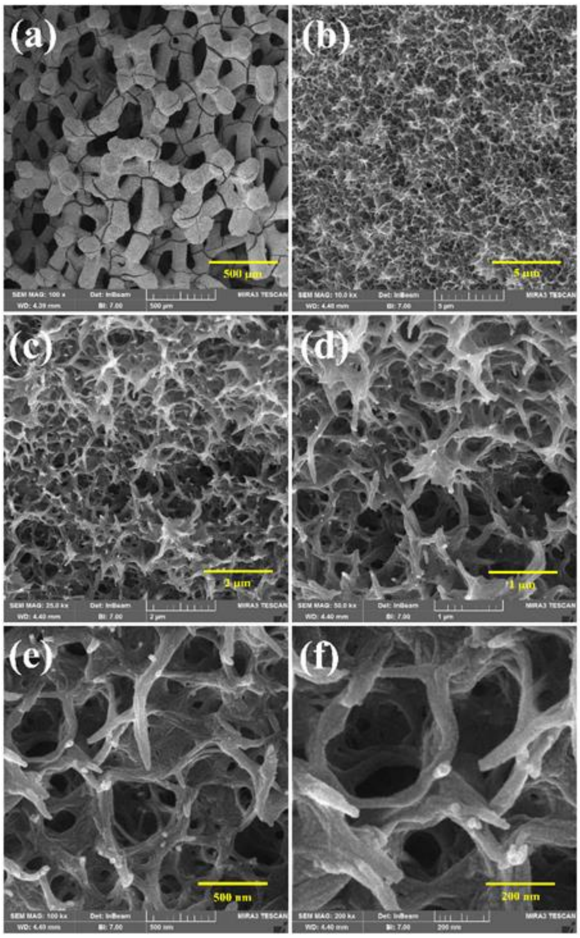

Fig. 4. FESEM images of the binder-free V_2O_5 electrode at various magnifications.

3.2. Electrochemical Measurements

The electrochemical performance of the electrodeposited binder-free V_2O_5 electrode in 2M $LiClO_4$ electrolyte was evaluated at room temperature. Figure 5 illustrates the cyclic voltammetry curves at various scan rates from 50 to 500 mV s^{-1} in the three-electrode system. The obtained cyclic voltammograms have a quasi-rectangular shape containing redox peaks, indicating the pseudocapacitive characteristic of the V_2O_5 electrode in lithium perchlorate electrolyte, which is accomplished by a fast reversible electrochemical process at the active material/ electrolyte interface. The nature of all CV plots is non-rectangular but symmetric, which reveals the pseudocapacitive nature of the V_2O_5 electrode. The pseudocapacitive behavior of the V_2O_5 electrode is induced as a result of the intercalation/de-intercalation mechanism of lithium ions within the crystal structure of vanadium oxide according to the following electrochemical reaction [19]:

$$V_2O_5 + xLi^+ + xe^- \leftrightarrow Li_xV_2O_5 \quad 0 < x < 1 \tag{3}$$

As a result of this intercalation/de-intercalation reaction, the valence of vanadium is shifted between V^{5+} and V^{4+} and therfore electron is stored in the active material. In other words, the valence of vanadium in V_2O_5 is 5+. However, with lithium ion intercalation, the active material is converted to LiV_2O_5, in which the valence of vanadium is 4+. Also, the shape of the voltammograms remains almost unchanged with increasing potential scan rate even up to a very high value of 400 mV s^{-1}, indicating the superior rate performance of the V_2O_5 electrode.

The combination of the faradaic pseudocapacitive behavior and the electric double layer, together with the high current response and the acceptable area of the CV curve, introduces this electrode as a suitable option for application in SCs.

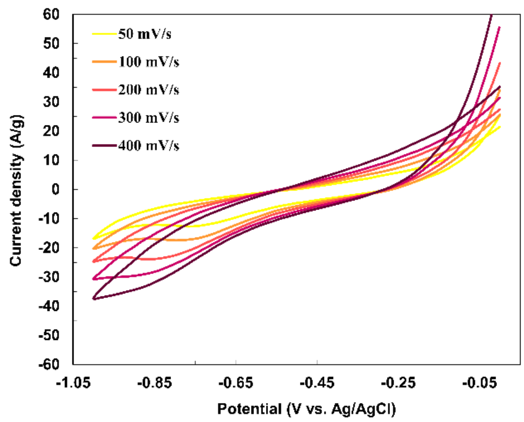

Fig. 5. CV curves of the V_2O_5 electrode at various scan rates.

In order to measure the specific capacitance (C_s) of the V_2O_5 electrode, galvanostatic charge-discharge studies were performed in the three-electrode system. Figure 6a depicts the GCD curves of the electrode at current rates from 1 to 10 A g^{-1}. As can be clearly seen, the curves have a nearly triangular shape, indicating the pseudocapacitive behavior of the V_2O_5 electrode along with some electrical double-layer capacitive characteristics. It is also observed that the GCD curves exhibit an IR drop, which occurs due to the charge transfer resistance.

The C_s of the V_2O_5 electrode was calculated based on the electrode discharge time according to the following equation [3], and the results are shown in Figure 6b:

$$C_s=(i\times\Delta t)/(m\times\Delta V) \tag{4}$$

where i is the charge and discharge current, Δt is the discharge time of the electrode to a voltage of 0 V (vs. Ag/AgCl), ΔV is the working potential window, which is equal to 1 V, and m is the mass of the electrode material. As shown in Figure 6b, the V_2O_5 electrode exhibited high specific capacitances of 496, 372, 247, and 179 F g^{-1} at current densities of 1, 2, 5, and 10 A g^{-1}, respectively. In addition, the capacitance retention with a 10-fold increase in current rate was calculated to be 36.1%.

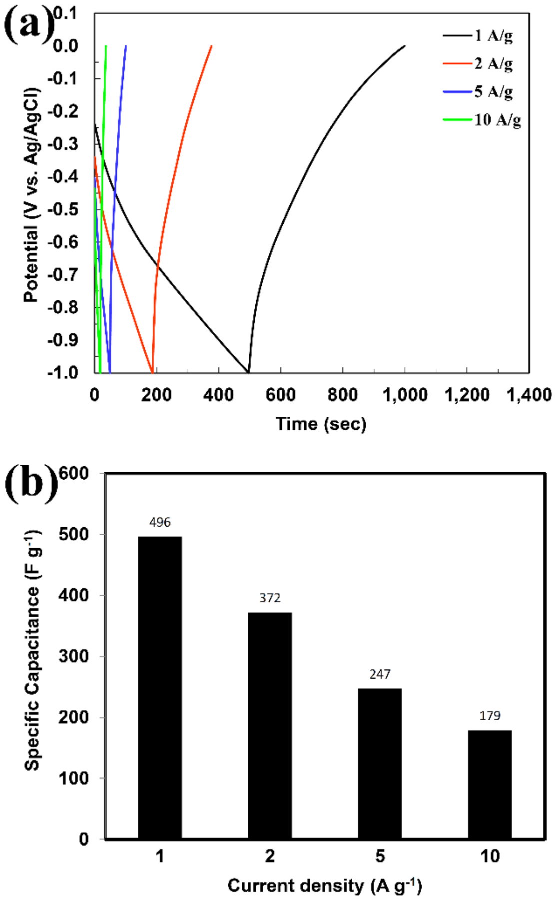

Fig. 6. (a) GCD profiles of the V_2O_5 electrode at various current rates; (b) C_s as a function of current rate.

The electrochemical impedance technique is an ideal method for measuring the internal resistance of the electrode as well as the diffusion resistance of electrolyte ions within the electrode structure. Figure 7a shows the Nyquist plot of the V_2O_5 electrode measured over the frequency range of 100 kHz-100 mHz with the amplitude of the sinusoidal signal of ±10 mV at open circuit voltage (OCV). At the open circuit voltage, the dominant electrochemical reaction is the charge transfer process resulting from the diffusion of lithium ions within the electrode structure and their intercalation/de-intercalation in the active material. It can be clearly seen that the Nyquist plot consists of a depressed semicircle in the high-frequency region and a sloping line in the low-frequency region. The sloping line, known as the Warburg impedance, is related to the diffusion rate of Li^+ ion, and the diameter of the semicircle is related to the charge transfer resistance. By fitting the Nyquist curve with the circuit depicted in the inset of Figure 7a, the charge transfer resistance is determined as 9.1 Ω, which is low compared to conventional electrodes.

Also, the diffusion coefficient of Li^+ within the V_2O_5 structure was measured using the Warburg region line and according to the following equation [21]:

$$D = 0.5\left(\frac{RT}{An^2F^2\sigma_w C}\right)^2 \tag{5}$$

where R is the gas constant (8.314 J mol^{-1} K^{-1}), T is the temperature (298 K in this work), A is the exposed area of the electrode, n is the number of electrons per molecule involved in the reaction, F is Faraday's constant (96,500 C mol^{-1}), C is the concentration of sodium ions in the electrolyte and σ_w is the Warburg factor, which is calculated based on the following equation:

$$Z_{re} = R_D + R_L + \sigma_w \omega^{-1/2} \tag{6}$$

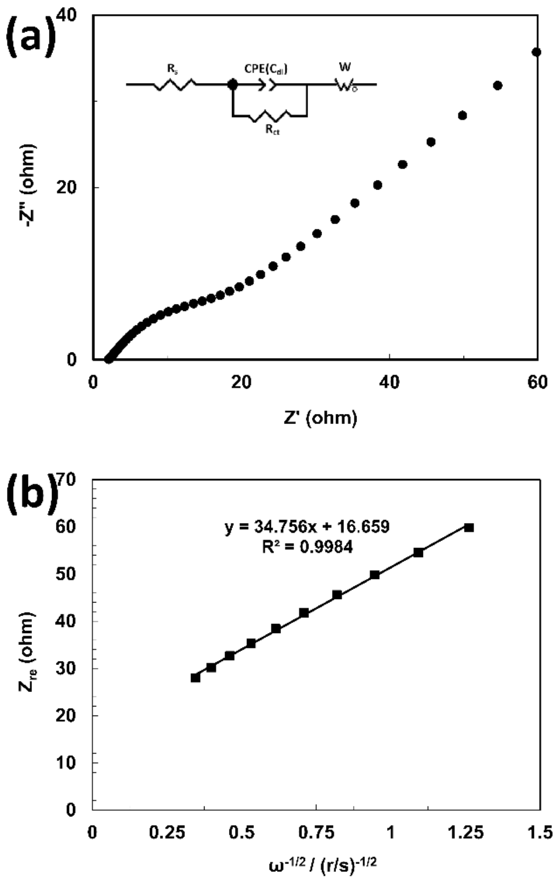

Fig. 7. (a) Nyquist curve of the V_2O_5 electrode; (b) The relationship between Z_{re} and $\omega^{-1/2}$.

To measure σ_w, it is sufficient to plot the real resistance values in the Warburg region against the reciprocal square root of the angular frequencies and obtain its slope, which is the Warburg factor. Based on the slope of the fitted line in Figure 7b and calculations performed using Equation 5, the diffusion coefficient of Li^+ in the V_2O_5 electrode is calculated to be $7.32 \times 10^{-12}\ cm^2 s^{-1}$.

Cyclic stability is a fundamental factor for the application of energy storage electrodes in batteries and supercapacitors. The capacitance loss in successive charge-discharge cycles is usually due to the internal stress induced by the continuous expansion and contraction resulting from intercalation/de-intercalation of Li^+ ions. For this purpose, the cycling performance of the binder-free V_2O_5 electrode was investigated for 2000 cycles at 5 A g^{-1}. As can be seen in Figure 8, after 2000 cycles, the electrode retained 85.2% of its initial capacitance, indicating its good cyclability. The acceptable cycling of the prepared vanadium oxide electrode can be related to its mesoporous structure, which damps the stresses induced in the faradaic charge-discharge processes.

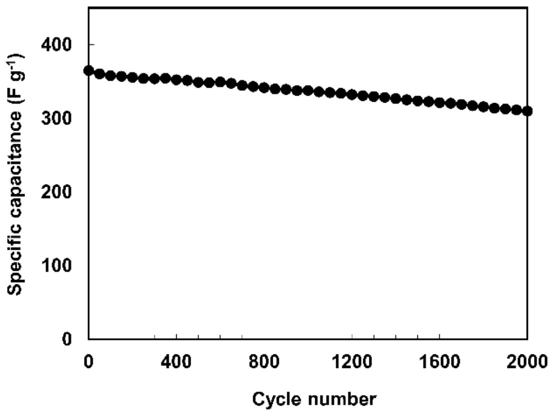

Fig. 8. Cyclability of the V_2O_5 electrode at 5.0 A g^{-1}.

4. Conclusions

In summary, a binder-free mesoporous vanadium oxide electrode was fabricated by a two-step strategy including anodic electrodeposition followed by calcination. The morphological, structural, and surface characteristics of the fabricated electrode, as well as its supercapacitive performance, were carefully evaluated. The results indicated a mesoporous and uniform structure of the V_2O_5 layer. Also, an acceptable energy storage performance was obtained for the prepared electrode, including a high capacitance of 496 F g^{-1} at 1 A g^{-1}, a suitable rate capability with a capacity retention of 36.1%, and good cyclability. The mesoporous structure of the V_2O_5 electrode material, in addition to removing the binder in the during electrode preparation, facilitated access of electrolyte ions to the active material and reduced the internal resistance of the electrode, all of which improved its electrochemical performance.

Funding Statement

The authors appreciate the Malayer University for its financial support (Grant NO. 84/9-378).

Conflicts of Interest

The authors declare that they have no known competing financial interests or personal relationships that could have appeared to influence the work reported in this paper.

Authors Contribution Statement

Mahdi Kazazi contributed to supervision, writing—review and editing, project administration, methodology, investigation, experimental design, and conceptualization.

Soheila Kazemi contributed to data analysis, data curation and experimentation, and writing original draft.

Behzad Koozegar Kaleji contributed to supervision, writing—review and editing.

References

[1] Kazazi, M., Mirzaie, M. And Rahimi Junaqani, J., 2024. Pseudocapacitive performance of cobaltite and nickel cobaltite electrodes fabricated by layer-by-layer chemical deposition method. *Progress in Physics of Applied Materials*, *4*, pp. 145-151.

[2] Huseyin, A. and Salih Salih, A.J., 2025. Batteries and supercapacitors: An analytical perspective on electrode materials and performance challenges. *Journal of Alloys and Compounds*, *1037*, pp. 181972.

[3] Kamleshbhai Patel, K., Singhal, T., Pandey, V., Sumangala, T.P. and Sreekanth, M.S., 2021. Evolution and recent developments of high performance electrode material for supercapacitors: A review. *Journal of Energy Storage*, *44,* pp. 103366.

[4] Wei, Y.M., Kumar, K.D., Zhang, L. and Li, J.F., 2025. Pseudocapacitive materials for energy storage: properties, mechanisms, and applications in supercapacitors and batteries. *Frontiers in Chemistry*, *13*, pp. 1636683.

[5] Bhojane, P., 2022. Recent advances and fundamentals of Pseudocapacitors: Materials, mechanism, and its understanding. *Journal of Energy Storage*, *45*, pp. 103654.

[6] Li, Z., Xu, M., Xia, Y., Yan, Z., Dai, J., Hu, B., Feng, H., Xu, S. and Wang, X., 2025. High-frequency supercapacitors surpassing dynamic limit of electrical double layer effects. *Nature Communications*, *16*, pp. 3704.

[7] Conway. B.E. and Pell, W.G., 2003. Double-layer and pseudocapacitance types of electrochemical capacitors and their applications to the development of hybrid devices. *Journal of Solid State Electrochemistry*, *7*, pp. 637–644.

[8] Ma, D., Han, C., Liu, B., Chen, J., Wu, M. and Guan, D., 2024. Vanadium Oxide-Based Electrode Materials for Advanced Supercapacitors: A Review. *Energy & Fuels*, *38,* pp. 10494–10516.

[9] Karthikeyan, S., Sowbakkiyavathi, E.S., Sindhuja, M. and Sukeri, A., 2025. Enhanced energy storage performance of two-dimensional vanadium oxide nanosheets for supercapacitors. *Ionics*, *31*, pp. 6145–6153.

[10] Yan, Y., Li, B., Guo, W., Pang, H. and Xue, H., 2016. Vanadium based materials as electrode materials for high performance supercapacitors. *Journal of Power Sources*, *329*, pp.148-169.

[11] Wang, A.Y., Chaudhary, M. and Lin, T.W., 2019. Enhancing the stability and capacitance of vanadium oxide nanoribbons/3D-graphene binder-free electrode by using $VOSO_4$ as redox-active electrolyte. *Chemical Engineering Journal, 355*, pp. 830-839.

[12] Yadav, A.D., Patil, R. and Patil, S.P., 2025. Exploring the frontiers of energy storage: vanadium oxide nanocomposites in supercapacitor technologies. *Ionics, 31*, pp. 41–66.

[13] Pullanchiyodan, A., Joy, R., Sreeram, P., Raphael, L.R., Das, A., Balakrishnan, N.T.M., Ahn. J.H., Vlad. A., Sreejith, S. and Raghavan, P., 2023. Recent advances in electrospun fibers based on transition metal oxides for supercapacitor applications: a review. *Energy Advances, 2*, pp. 922-947.

[14] Raza, A., Khan, I.A. and Farid, A., 2026. Enriched pseudocapacitive performance of CVD deposited $MoSe_2/MoS_2$ heterostructured binder free nanospheres for asymmetric supercapacitor applications. *Journal of Physics and Chemistry of Solids, 208*, pp. 113138.

[15] Shivasharma, T.K., Upadhyay, N., Deshmukh, T.B. and Sankapal, B.R., 2023. Exploring Vacuum-Assisted Thin Films toward Supercapacitor Applications: Present Status and Future Prospects. *ACS Omega, 41*, pp. 37685-37719.

[16] Asen, P., Shahrokhian, S. and Iraji zad, A., 2017. One step electrodeposition of V_2O_5/polypyrrole/graphene oxide ternary nanocomposite for preparation of a high performance supercapacitor. *International Journal of Hydrogen Energy, 40,* pp. 21073-21085.

[17] Abebe, E.M. and Ujihara, M., 2022. Simultaneous Electrodeposition of Ternary Metal Oxide Nanocomposites for High-Efficiency Supercapacitor Applications. *ACS Omega, 7*, pp. 17161-17174.

[18] Aamir, A., Ahmad, A., Khan, Y., Rehman, Z.U., Ain, N.U., Shah, S.K., Mehmood, M. and Zaman, B., 2020. Electrodeposited thick coatings of V_2O_5 on Ni foam as binder free electrodes for supercapacitors. *Bulletin of Materials Science, 43*, pp. 273.

[19] Velayutham, R., Manikandan, R., Raj, C.J., Kale, A.M., Kaya, C., Palanisamy, K. and Kim, B.C., 2021. Electrodeposition of vanadium pentoxide on carbon fiber cloth as a binder-free electrode for high-performance asymmetric supercapacitor. *Journal of Alloys and Compounds, 863*, pp. 158332.

[20] Latha, K., Anbuselvi, S., Periasamy, P., Sudha, R. and Velmurugan, D., 2021. Structural and electrochemical investigation of novel hybridized MnO_2/V_2O_5 nanocomposites prepared by one-step microwave-assisted method for electrochemical supercapacitor application. *Journal of Materials Science: Materials in Electronics, 32,* pp. 23293-23308.

[21] Kazazi, M. and Mirzaie, R., 2026. Anodic Electrodeposition of NiOOH on 3D rGO Framework for High-Performance Pseudocapacitors. *JOM, 78*, pp. 52-64.